

**Improved dust  
emission scheme in  
ECHAM5-HAM GCM**

T. Cheng et al.

# An improvement on the dust emission scheme in the global aerosol-climate model ECHAM5-HAM

**T. Cheng<sup>1,3</sup>, Y. Peng<sup>1,4</sup>, J. Feichter<sup>1</sup>, and I. Tegen<sup>2</sup>**

<sup>1</sup>Max-Planck-Institute for Meteorology, Bundesstr. 53, 20146, Hamburg, Germany

<sup>2</sup>Leibniz-Institute for Tropospheric Research, Permoserstrasse 15, 04318 Leipzig, Germany

<sup>3</sup>Department of Environmental Science and Engineering, Fudan University, Shanghai, 200433, China

<sup>4</sup>Canadian Centre for Climate Modeling and Analysis, 3964 Gordon Head Road, Victoria, B.C., V8N 3X3, Canada

Received: 30 August 2007 – Accepted: 21 September 2007 – Published: 27 September 2007

Correspondence to: Y. Peng (yiran.peng@ec.gc.ca)

Title Page

Abstract

Introduction

Conclusions

References

Tables

Figures

⏪

⏩

◀

▶

Back

Close

Full Screen / Esc

Printer-friendly Version

Interactive Discussion

## Abstract

Formulation of the dust emission scheme in the global aerosol-climate modeling system ECHAM5-HAM has been improved. Modifications on the surface aerodynamic roughness length, soil moisture and East-Asian soil properties are included in the parameterization, which result in a large impact on the threshold wind friction velocity for aeolian erosion and thus influence the simulated dust emission amount. The annual global mean of dust emission in the year 2000 is reduced by 76.5% and 2.2%, respectively, due to changes in the aerodynamic roughness length and the soil moisture. An inclusion of detailed East-Asian soil properties leads to an increase of 16.6% in the annual global mean of dust emission, which exhibits mainly in the arid and semi-arid areas of northern China and southern Mongolia. Reasonable values of annual global mean of dust emission, dust burden and total aerosol optical thickness can be obtained in the improved model. In addition, measurements of the surface dust concentrations are collected in dust source regions of East Asia, and verify a more realistic spatial distribution of dust emission in the improved model.

## 1 Introduction

Atmospheric aerosol is an important forcing factor in the global climate system. However, considerable uncertainties still exist in the estimates of direct and indirect effects of aerosols on the earth radiation budget and global climate changes (IPCC, 2001). Among several atmospheric aerosol species, mineral dust is one of the largest contributors to the global aerosol loading and has strong impacts on regional and global climates (Tegen et al., 1996), marine and terrestrial ecosystems (Martin et al., 1988; Chadwick et al., 1999), as well as the long-term climate trends (Petit et al., 1990, 1999).

A global aerosol-climate model can help to understand the complex aerosol cycle for past, present and future conditions, to distinguish natural from anthropogenic aerosol sources and to identify the effect of specific aerosol components on the global climate

ACPD

7, 13959–13987, 2007

## Improved dust emission scheme in ECHAM5-HAM GCM

T. Cheng et al.

Title Page

Abstract

Introduction

Conclusions

References

Tables

Figures

⏪

⏩

◀

▶

Back

Close

Full Screen / Esc

Printer-friendly Version

Interactive Discussion

EGU

system. The global simulation of dust cycle is able to reproduce the first-order patterns of dust transport and deposition under modern climate conditions (Tegen et al., 1996, 2002). However, none of the current models can correctly simulate the dust emission, transportation, wet and dry depositions at the same time in different dust source regions of the globe, which is probably attributed to oversimplifications of dust relevant processes parameterized in models.

The aerosol-climate modeling system ECHAM5-HAM predicts the ensemble of micro-physically interacting internally-mixed and externally-mixed aerosol populations as well as their size distribution and composition (Stier et al., 2005). The model can appropriately estimate the global distribution, transportation and climate impact of dust aerosols. Nevertheless, the parameterization of dust emission in ECHAM5-HAM is still rather crude. Some key parameters such as the surface roughness, soil moisture and soil properties at various locations are not very well included. Therefore further modifications on the dust emission scheme are expected in order to simulate the mineral dust aerosols more realistically.

In this study, we present an improved dust emission scheme for application into the ECHAM5-HAM, which incorporates updates of the surface aerodynamic roughness length, soil moisture and East-Asian soil properties. Objectives of this work are to include a more physically based parameterization of the threshold wind friction velocity, and to obtain a more realistic surface dust emission than previously. In Sect. 2, we describe the three modifications of the improved dust emission scheme applying into ECHAM5-HAM. Results from model simulations with the improved scheme as well as comparisons with the previous simulation and measurements are shown in Sect. 3. Concluding remarks and discussions are given in Sect. 4.

## 2 Improvement on the dust emission scheme in ECHAM5-HAM

The dust emission driven by wind in arid and semi-arid areas is a non-linear physical process, which depends on both surface features and meteorological conditions in the

### Improved dust emission scheme in ECHAM5-HAM GCM

T. Cheng et al.

Title Page

Abstract

Introduction

Conclusions

References

Tables

Figures

⏪

⏩

◀

▶

Back

Close

Full Screen / Esc

Printer-friendly Version

Interactive Discussion

## Improved dust emission scheme in ECHAM5-HAM GCM

T. Cheng et al.

Title Page

Abstract

Introduction

Conclusions

References

Tables

Figures

◀

▶

◀

▶

Back

Close

Full Screen / Esc

Printer-friendly Version

Interactive Discussion

potential source areas. The emission flux of moveable soil-derived particles is a power function of the wind friction velocity, and occurs only if the threshold of wind friction velocity is exceeded. The threshold value is primarily a function of the soil size distribution, the roughness of erodible surface (Marticorena and Bergametti, 1995), and the soil moisture (Fécan et al., 1999). The developed dust emission scheme and the required input parameters for a large-scale model application are already well described by Marticorena et al. (1997a).

In the aerosol-climate model ECHAM5-HAM, emission of mineral dust depends on the online prognostic wind speed at 10 meter above the surface and the prescribed surface feature of soils. The global soil texture is classified into 12 types to represent soil properties in the preferential dust source areas, which areas are derived from an explicit simulation of paleological lake beds (Tegen et al., 2002). The soil texture of ECHAM5-HAM specifies coarse sand, medium or fine sand, silt and clay populations, but neglects the super-coarse mode particles. The emission scheme is applied into the insoluble accumulation and coarse modes with mass-median radii of  $0.37 \mu\text{m}$  and  $1.75 \mu\text{m}$  and standard deviations of 1.59 and 2.00 respectively (Stier et al., 2005).

### 2.1 Surface aerodynamic roughness length

The dust emission scheme is related to a parameterization of the threshold wind friction velocity, which is a function of the size of erodible soil particles ( $D_p$ ), the local aerodynamic roughness length of overall surface ( $Z_0$ ), and the local aerodynamic roughness length of erodible or uncovered surface ( $z_{0s}$ ). The size-dependent threshold of wind friction velocity ( $U_t^*$ ) for dust emission is calculated as:

$$U_t^*(D_p, Z_0, z_{0s}) = \frac{U_t^*(D_p)}{f_{\text{eff}}(Z_0, z_{0s})} \quad (1)$$

$$f_{\text{eff}}(Z_0, z_{0s}) = 1 - \left[ \ln \left( \frac{Z_0}{z_{0s}} \right) / \ln \left( 0.35 \left( \frac{10}{z_{0s}} \right)^{0.8} \right) \right] \quad (2)$$

13962

Where  $f_{\text{eff}}$  is the efficient friction velocity ratio defined as the ratio of local to total friction velocity on the basis of a drag partition scheme developed by Marticorena and Bergametti (1995). This parameterization was proved to agree with the wind tunnel and in-situ measurements of threshold wind friction velocities taken over a variety of natural erosion surfaces (Gillette et al., 1982; Marticorena et al., 1997a). However, the application of such a physically-based parameterization in a large scale model is limited due to the lack of global information characterizing the surface features in arid and semi-arid areas, particularly the surface aerodynamic roughness length  $Z_0$ .

The aerodynamic roughness length  $Z_0$  is defined as the height above a surface at which the wind profile is assumed to be zero. It relates to both quantities of potentially eroded material and the minimum wind speed required for raising the dust particles (Gillette and Passi, 1988). The threshold velocity  $U_t^*$  to initiate the dust emission is increased in areas with higher  $Z_0$  compared to smooth surfaces (cf., Eqs. 1 and 2). The enhanced  $Z_0$  also reduces the wind friction velocity and decreases the dust emission flux. Previous global model of dust cycle either uses a prescribed constant  $Z_0$  field over the globe (Tegen et al., 2002), or calculates the dust emission flux directly from the model predicted surface wind speed instead of the wind friction velocity, implicitly assuming a constant  $Z_0$  (Ginoux et al., 2001). This is because few  $Z_0$  data is available in arid and semi-arid areas of the globe.

Recently, Marticorena et al. (2004) mapped the surface roughness length  $Z_0$  in North Africa based on measurements with the POLarization and Directionality of the Earth's Reflectance (POLDER) instrument on board the ADvanced Earth Observation Satellite (ADEOS) platform. The resulted  $Z_0$  was derived from an empirical relationship between the satellite observed bidirectional reflectances and estimates of surface roughness from in-situ measurements. Following a similar method, Prigent et al. (2005) derived a global  $Z_0$  field from observations in arid and semi-arid areas of the globe, according to measurements with the European Remote Sensing (ERS) satellite scatterometer.

In the previous dust emission scheme of ECHAM5-HAM, the aerodynamic roughness length  $Z_0$  was fixed as a constant value equal to the smooth aerodynamic rough-

---

**Improved dust emission scheme in ECHAM5-HAM GCM**T. Cheng et al.

---

[Title Page](#)[Abstract](#)[Introduction](#)[Conclusions](#)[References](#)[Tables](#)[Figures](#)[⏪](#)[⏩](#)[◀](#)[▶](#)[Back](#)[Close](#)[Full Screen / Esc](#)[Printer-friendly Version](#)[Interactive Discussion](#)

ness length  $z_{0s}$  of 0.001 cm. The globally constant  $Z_0$  field is invariant to time and location, and thus does not account for the potential changes related to the vegetation cycle or anthropogenic influences. In the improved dust emission scheme, we take 12 monthly mean  $Z_0$  fields derived in Prigent et al. (2005) and re-grid the data to the same horizontal resolution as which is used for running ECHAM5-HAM (T63 in this study, cf., Sect. 3). Figure 1 presents the updated annual mean  $Z_0$  field with the horizontal resolution of T63 (roughly  $1.8^\circ \times 1.8^\circ$ ). The updated  $Z_0$  is generally higher than 0.01 cm in all seasons and in most of the dust source areas, which is increased by one order of magnitude comparing to the previously fixed value of 0.001 cm.

## 2.2 Soil moisture

Fécan et al. (1999) parameterized the influence of soil moisture on the threshold wind friction velocity, which is a function of gravimetric soil moisture  $w$ , and soil residual moisture  $w'$ .

$$\frac{U_{tw}^*}{U_t^*} = 1 \quad \text{for } w < w' \quad (3)$$

$$\frac{U_{tw}^*}{U_t^*} = \left[ 1 + 1.21 (w - w')^{0.68} \right]^{0.5} \quad \text{for } w > w' \quad (4)$$

$$w' = 0.0014 \times (\% \text{clay})^2 + 0.17 \times (\% \text{clay}) \quad (5)$$

$U_t^*$  is the threshold wind velocity in dry soil conditions,  $U_{tw}^*$  is the threshold wind velocity including the effect of soil moisture conditions.  $w'$  can be obtained from the clay content with a unit of % (Fécan et al., 1999). In ECHAM5-HAM we take values of  $w'$  from Werner et al. (2002) for 12 prescribed soil types.

We include the parameterization of the soil moisture effect (Eqs. 3 and 4) into the improved dust emission scheme. The model predicted soil moisture  $w$  is obtained from the standard ECHAM5 output, and a soil particle density of  $2.65 \text{ g cm}^{-3}$  is used.

## Improved dust emission scheme in ECHAM5-HAM GCM

T. Cheng et al.

Title Page

Abstract

Introduction

Conclusions

References

Tables

Figures

◀

▶

◀

▶

Back

Close

Full Screen / Esc

Printer-friendly Version

Interactive Discussion

## 2.3 East-Asian soil properties

East Asia is one of the largest dust source regions in the globe. For example, arid and semiarid lands occupy 3.57 million km<sup>2</sup> in China, distributed from west to east as the Taklimakan, Gurbantunggut, Tsaidam Basin, Kumutage, Badian Juran, Tengger, Ulan Buh, Hobq, Mu Us deserts and other small deserts. Desert plains and Gobi also occupy a large portion of Mongolia. Over these vast areas, dust storms are frequent and sometimes severe, especially from late spring to early summer. Moreover, an ongoing desertification due to overgrazing and unreasonable land use has been identified in China (Zha and Gao, 1997) and Mongolia (Natsagdorj et al., 2003), which results in additional dust sources.

In the previous emission scheme of ECHAM5-HAM, soil texture was derived from the Food and Agriculture Organization (FAO) of United Nations Educational, Scientific, and Cultural Organization soil map of the World (Zobler, 1986; Tegen et al., 2002), which results in a significant underestimate of the dust emission amount in East Asia. Recently many studies investigate East-Asian soil properties into details. The map of updated soil types in China and Mongolia is obtained according to the spatial distribution of geographic land and surface vegetation types, as well as in-situ measurements of soil particle size and soil textures (Xu et al., 2006). Soils in China and Mongolia (75° to 130° N, 34° to 50° E) are categorized into 5 groups namely Taklimakan, Loess, Gobi, desert and sand land, and other mixture soils (Table 1). The area percentage of the 5 soil types in the model grid box at East Asia are plotted in Fig. 2 with a horizontal resolution of 1.8° × 1.8°.

Two major soil properties are required for implementing the dust emission scheme into models: (1) the soil size distribution of in-situ erodible grains and aggregates; (2) the soil texture. Based on intensive samplings in the main Chinese arid areas, Mei et al. (2004) and Yang et al. (2001) have determined the typical micro-aggregated size distribution of surface erodible soils following the approach of Chatenet et al. (1996). For each of these 5 soil type, the mass-size distribution is fitted to two lognormal func-

### Improved dust emission scheme in ECHAM5-HAM GCM

T. Cheng et al.

Title Page

Abstract

Introduction

Conclusions

References

Tables

Figures

◀

▶

◀

▶

Back

Close

Full Screen / Esc

Printer-friendly Version

Interactive Discussion

tions in fine and coarse modes, with respective parameters of mass median diameter (MMD), standard deviation ( $\sigma$ ) and mass fraction (P). It is, however, essential to note that the size of Chinese desert soil particles in both fine and coarse modes are significantly smaller than that of Saharan soils (Chatenet et al., 1996), which explains the underestimation of emission amount in previous simulations with ECHAM5-HAM. Table 1 summarizes the statistical parameters (MMD,  $\sigma$  and P for fine and coarse modes respectively) of 5 updated soil types in potential dust source areas of China and Mongolia.

In addition to the soil size distribution, Mei et al. (2004) investigated the soil textures in the corresponding Chinese arid areas. The overall median clay contents of Chinese soils (Laurent et al., 2006) are comparable to the North American (Marticorena et al., 1997b) and Saharan (Chatenet et al., 1996) soils. Ding et al. (1999) measured the soil clay contents of Chinese loess and sandy loess. A typical value of 17% is taken as the representative for the clay content of loess (Table 1). Similarly, the silt content, the ratio of vertical to horizontal dust fluxes ( $\alpha$ ) and the soil residual moisture ( $w'$ ) for 5 updated soil types are obtained (Laurent et al., 2006), and summarized in Table 1. The updated data of soil types, size distributions and soil textures in East-Asian dust source areas replace the previous input in the improved dust emission scheme of ECHAM5-HAM.

### 3 Results

#### 3.1 Evaluation on the improved dust emission scheme

ECHAM5-HAM simulations are performed for the year 2000 after a spin-up time of three months. Temperature, pressure and horizontal wind velocities are nudged to the ECMWF ERA40 reanalysis data. The model uses horizontal resolution of T63 and has 31 hybrid levels vertically. Seven experiments are run to examine the sensitivity of global dust emissions to modifications in the improved scheme. Case 0 is the reference simulation with the original dust emission scheme. Case 1 to case 3 are simulations

## Improved dust emission scheme in ECHAM5-HAM GCM

T. Cheng et al.

Title Page

Abstract

Introduction

Conclusions

References

Tables

Figures

◀

▶

◀

▶

Back

Close

Full Screen / Esc

Printer-friendly Version

Interactive Discussion

including the update of  $Z_0$ , soil moisture and East-Asian soil properties respectively. Case 4 is the simulation of ECHAM5-HAM with the improved dust emission scheme. In case 5 we artificially tune a parameter of wind stress correction factor (cf., Tegen et al., 2004) to reduce the threshold wind friction velocity, in order to obtain a reasonable global mean emission amount and a realistic spatial distribution of dust aerosols (Timmreck and Schulz, 2004). In case 6 we rerun the reference case with the tuned threshold wind velocity.

Table 2 lists the setup of seven simulations and the corresponding results as annual global means of dust emission amount, atmospheric dust burden, total aerosol optical thickness (AOT) and dust AOT. The inclusion of updated  $Z_0$  field and soil moisture results in 76.5% and 2.2% decreases of the dust emission amount, while the modified East-Asian soil properties lead to an increase of 16.6%. Changes in the dust burden, total AOT and dust AOT are similar to that of emission amount. The great reduction from case 0 to case 1 is due to the generally high  $Z_0$  in the updated field (cf., Fig. 1 and Sect. 2.1) and shows a similar trend with results in Laurent et al. (2005, 2006) and Tegen et al. (2004). The increase from case 0 to case 3 as a result of modified East-Asian soil properties leads to a better agreement with measurements, as will be seen in Sect. 3.2.

The more physically-based dust emission scheme reduces the emission amount dramatically (case 4 vs. case 0). Therefore the wind stress correction factor has to be lowered in order to decrease the threshold wind velocity and to enhance the emission (same approach as in Timmreck and Schulz, 2004). As the wind stress correction factor varies from 0.86 to 0.56 a reasonable emission amount of around  $1670.7 \text{ Tg yr}^{-1}$  can be obtained (case 5), which falls in the range of 1000 to  $3000 \text{ Tg yr}^{-1}$  as estimated by IPCC (2001). It also agrees to the median of model estimates in AeroCom (<http://nansen.ipsl.jussieu.fr/AEROCOM/>), which is  $1770 \text{ Tg yr}^{-1}$ . In case 5 the total AOT is 0.15, which falls in the range of 0.116 to 0.155 suggested by AeroCom model inter-comparison (Kinne et al., 2006). The total AOT is also similar to the estimated value of 0.14 as derived from AERONET measurements (Kinne et al., 2003).

---

**Improved dust emission scheme in ECHAM5-HAM GCM**T. Cheng et al.

---

Title Page

Abstract

Introduction

Conclusions

References

Tables

Figures

◀

▶

◀

▶

Back

Close

Full Screen / Esc

Printer-friendly Version

Interactive Discussion

Figure 3 shows the percentage differences between sensitivity simulations and the reference simulation in terms of the annual mean dust emission amount. Large decreases exhibit globally due to the high values of  $Z_0$  in the updated field (case 1 vs. case 0), while great reduction occurs in North America desert and part of Sahara, Australia, India and Middle East deserts. The change of soil moisture parameterization results in decreases in part of North America, Australia, South Africa and Middle East deserts, as well as small increases in India and Middle Asia (case 2 vs. case 0). An exclusive enhancement in arid and semi-arid areas of northern China and southern Mongolia (case 3 vs. case 0) is caused by the modified East-Asian soil properties. It is worth mentioning that the general pattern of dust seasonal cycle is not significantly influenced by the improved emission scheme (not shown). The decrease due to the updated  $Z_0$  field dominates and contributes to the global reduction from case 0 to case 4, although modified East-Asian soil properties are responsible for an enhancement in the specific region. Lowering the wind stress correction factor from 0.86 to 0.56 leads to an overall large increase (case 6 vs. case 0), which compensates the reduction from the improved emission scheme.

There are few observations of the global dust distribution and no direct measurements of dust emissions are available. Nevertheless, we compare the simulated dust mass concentration at the lowest model level with the surface measurements in multiple remote marine sites (similar to the comparison in Stier et al., 2005), in order to evaluate the improved dust emission scheme in ECHAM5-HAM. Figure 4 presents a comparison of annual mean surface dust mass concentrations (data are listed in Table 3). Measurements are averaged from multiyear observations at 21 remote marine sites by University of Miami network. Model results are derived from ECHAM5-HAM simulations in year 2000 with and without the improved dust emission scheme (case 5 and case 0 in Table 3 respectively). The mineral dust mass concentrations of Miami network were derived from the measured aluminum concentration in samples of total suspended particulate matter (TSP) on the assumption that mineral dust aerosols have an aluminum content equal to that of average soils, which is suggested to be 8%

**Improved dust emission scheme in ECHAM5-HAM GCM**

T. Cheng et al.

[Title Page](#)[Abstract](#)[Introduction](#)[Conclusions](#)[References](#)[Tables](#)[Figures](#)[⏪](#)[⏩](#)[◀](#)[▶](#)[Back](#)[Close](#)[Full Screen / Esc](#)[Printer-friendly Version](#)[Interactive Discussion](#)

(Prospero, 1999). The dust mass concentrations are generally underestimated by the model. Particularly low values of model predictions are noticeable (Note that Fig. 4 uses the logarithm scale. Some model estimates are below 0.01 but all measurements are above 0.1). One possible explanation is that model simulations are limited in the year 2000 while measurements are climatologically. Moreover, simplifications of the dust relevant processes in the model, e.g., the neglect of super coarse mode emission, an overestimation of sink processes for example an excessive microphysical aging, could potentially contribute to this large discrepancy.

Despite the large discrepancy in the individual site, results of case 5 show a better agreement to the measurements on average (see average values in Table 3 and correlation coefficients of Fig. 4). Including the improved dust emission scheme in ECHAM5-HAM raises the predicted surface dust concentrations, approaching to the measured values in most of northern hemisphere sites, especially in East Asia and the pacific islands (cf., data and locations in Table 3). However, case 5 still underestimates the surface dust concentrations for most of southern hemisphere sites, which could be attributed to unrealistic soil properties and underestimation of wind speed in this region in the model.

### 3.2 Validation on East-Asian dust emission

The atmospheric visibility is affected by the presence of aerosols and water vapor. During a dust episode, it is reasonable to assume that dust aerosol plays a determining role and thus the dust concentration can be estimated from visibility measurements. As one of the regular weather station records, visibility data provides good spatial and temporal coverage in China during recent years. We derive the surface dust concentration from selected visibility records, following the empirical relationships in Shao et al. (2003). The visibility data in non-dusty days are excluded, in order to rule out the impacts of other aerosol species. Note that the derived dust concentration from visibility observations may overestimate the realistic dust amount to some extent, due to the impact of air moisture on visibility. However, the empirical coefficients and the sub-

**Improved dust emission scheme in ECHAM5-HAM GCM**

T. Cheng et al.

Title Page

Abstract

Introduction

Conclusions

References

Tables

Figures

◀

▶

◀

▶

Back

Close

Full Screen / Esc

Printer-friendly Version

Interactive Discussion

jective observations on visibility introduce additional uncertainties. The derived dust concentrations exhibit a certain spatial pattern and can be a validation on the model simulation results in Asian area.

Figure 5 shows a comparison of monthly mean surface dust concentration in April of 2000 between the observed data derived from visibility and ECHAM5-HAM simulation results of case 0 and case 5. Dust storm prevails and dust activities are highly frequent in spring, therefore, the derived data are more reliable during this period. Both simulations can reproduce the pattern of dust source regions in Northern China. Over northwestern China, where the Tsaidam basin and the Kumutage desert are located, and in Northeast China, results of case 5 are more consistent with observations both in area extent and in magnitude. Case 5 also captures high dust concentrations along the boundary between Mongolia and Northeast China. In short, the improved dust emission scheme in case 5 enhances the model performance in China over dust source areas.

Few direct measurements of dust emission are available in East Asia. Alternatively, near-surface dust concentrations are measured in various locations of northern Asia by the China Dust Storm Research (ChinaDSR) during spring 2001 (Zhang et al., 2003), as part of the Asia Pacific Regional Aerosol Characterization Experiment (ACE-Asia), as well as by the Aeolian Dust Experiment on Climate (ADEC) from 2001 to 2004 (Kanai et al., 2005; Yabuki et al., 2005; Kim et al., 2003, 2006). Measurements taken from 16 stations are compared to model predictions in the corresponding time of 2001 and 2002 (Table 4 and Fig. 6). The selected stations are located in or downstream of the dust source regions (Table 4), with ten in China (Aksu, Dunhuang, Yulin, Changwu, Lanzhou, Shapotou, Inner-Mongolia, Beijing, Hefei and Qingdao), two in South Korea (Seoul and Gosan) and four in Japan (Tsukuba, Nagoya, Fukuoka and Naha). In these locations, dust mass concentrations are derived from the total aerosol loading and the average percentage of mineral matter, the latter is calculated from the sum of aluminum, silicon, calcium and iron oxides of intense aerosol samples following an empirical function (Solomon et al., 1989). ADEC data in Japan are almost continuous,

---

**Improved dust emission scheme in ECHAM5-HAM GCM**T. Cheng et al.

---

[Title Page](#)[Abstract](#)[Introduction](#)[Conclusions](#)[References](#)[Tables](#)[Figures](#)[⏪](#)[⏩](#)[◀](#)[▶](#)[Back](#)[Close](#)[Full Screen / Esc](#)[Printer-friendly Version](#)[Interactive Discussion](#)

whereas observations in China are carried out during dust events, thus high concentrations may be sampled (Kanai et al., 2005). Note that the measurement data show an average of dust mass concentration during the operation period.

The near-surface measurement data are compared to ECHAM5-HAM simulations of case 0 and case 5 in Fig. 6 (data are listed in Table 4). In most stations, results of case 5 are in better agreement with observations than case 0, especially in areas of East China, South Korea and Japan (cf., data in Table 4 and correlation coefficients of Fig. 6). Both comparisons in Fig. 5 and Fig. 6 validate the increase of dust emission in East Asia, which is mainly resulted from the modified soil properties in this region.

Although the improved dust emission scheme enables to produce a more realistic result in East Asia, the model still underestimates the dust surface concentration in source regions of northwestern China (cf., Fig. 5). One possible reason for the discrepancy is the coarse spatial resolution of ECHAM5-HAM grid box, in which the secondary dust sources, small scale synoptic systems, regional topography and geomorphology are not well solved. Most of the sandy deserts in China and Mongolia are located in closed basins, surrounded by stony hills and mountains. For example, the Taklimakan desert is in the closed basin of Tarim, the Gurban Tonggut desert lies in the basin of Junhhaar, both Badain Jaran and Tengger deserts are in the basin of Hanhai. Specific air circulations can be induced in such low-altitude locations. For instance, the Tarim basin is surrounded in three directions by Kulun Mounts, which is higher than 5000 m. Winds in this region are northeasterly except for the western margins (Sun, 2002). As a result, dusts from the Taklimakan desert remain confined in the southwestern slope of Kulun Mounts. On the other hand, the differences between model simulation and measurements are likely due to the lack of precise maps of surface features in East Asia, especially the soil clay content and erodible fraction of the surface.

---

**Improved dust emission scheme in ECHAM5-HAM GCM**T. Cheng et al.

---

[Title Page](#)[Abstract](#)[Introduction](#)[Conclusions](#)[References](#)[Tables](#)[Figures](#)[⏪](#)[⏩](#)[◀](#)[▶](#)[Back](#)[Close](#)[Full Screen / Esc](#)[Printer-friendly Version](#)[Interactive Discussion](#)

## 4 Concluding remarks and discussions

An improvement on the dust emission scheme is included in the global aerosol-climate modeling system ECHAM5-HAM. Modifications on the surface aerodynamic roughness length  $Z_0$ , soil moisture and East-Asian soil properties influence the calculation of threshold wind friction velocity for aeolian erosion. Changes in  $Z_0$  and soil moisture parameterization lead to decreases in the global dust emission amount. Updated East-Asian soil properties result in an enhancement of dust emission in arid and semi-arid areas of northern China and southern Mongolia. In global remote marine sites and specifically in Asia, the improved model shows better agreements than a previous model version, when comparing to in-situ measurements of the surface dust concentration.

Near-surface wind velocity is one key factor to control the saltation and erosion of soil particles. Dust emissions are particularly sensitive to small differences in wind speed because the parameterized emission flux is proportional to the third power of surface wind stress. We compare the monthly mean wind speeds observed in East Asian dust source regions with the simulated wind speeds at 10 m height above the surface in ECHAM5-HAM, during a dust active period of April, 2001 (results are not shown). The mean wind speed is generally underestimated by the model. The underestimation is even stronger where high wind speed is observed. Tegen et al. (2002) reported the similar underestimations on wind speed and on the maximum wind speed by the large scale model. The discrepancy between the ECHAM5 simulation and observed wind speeds could be a fundamental reason for the overall underestimation of dust surface concentrations shown in present results (e.g., Fig. 4). However, investigation on this problem is beyond the scope of the current study.

In the improved emission scheme we replace the constant  $Z_0$  with updated global  $Z_0$  field. Additionally, the smooth roughness length  $z_{0s}$  is assumed to be constant, which is about 1/30 of the coarser mass median diameter of soil size distribution in ECHAM5-HAM. It should be noted that the dust emission is very sensitive to  $z_{0s}$  in some specific

### Improved dust emission scheme in ECHAM5-HAM GCM

T. Cheng et al.

Title Page

Abstract

Introduction

Conclusions

References

Tables

Figures

⏪

⏩

◀

▶

Back

Close

Full Screen / Esc

Printer-friendly Version

Interactive Discussion

regions. For example in the Taklimakan desert, the coarser population represents a very small fraction (<3%) of soil size distribution (Mei et al., 2004).  $Z_0$  derived from satellite data in this desert (< $10^{-3}$  cm) is lower than in other sandy deserts (Laurent et al., 2005). Therefore,  $z_{0s}$  in the Taklimakan desert is likely to be derived as 1/30 of the finest mass median diameter, so that a part of smooth erodible surface can be transformed into a relatively rough and less erodible surface (Laurent et al., 2006). In order to better account for the surface feature in various locations, a map of  $z_{0s}$  will be helpful to further improve the global dust emission simulation.

Parameterized soil moisture effect in the improved emission scheme depends on the model predicted soil moisture, which is derived in the land surface scheme of ECHAM5. A homogeneous soil texture is assumed in the uppermost surface layer with a depth of 1.0 m and over the global land surface. As a result, the model is not able to simulate the low soil moisture content as measured in arid and semi-arid areas. For example, Van Den Hurk et al. (2000) proves that the soil moisture fields of ERA40 reanalysis data, which are derived in a land surface scheme including four prognostic soil layers with a homogeneous texture over the global land surface, does not match the low soil moisture contents measured in semi-arid areas such as Sahel. Although the general pattern and the seasonal cycle of dust emissions are not significantly influenced by the soil moisture, the moisture content of superficial soil layer contributes to dust emission in source regions. Therefore, a soil moisture field derived from a more realistic land surface scheme will help to understand the impact of climatic factors, such as precipitation, on dust emissions.

Dust emissions are in response to near-surface wind velocity, land surface features, soil properties and moisture content directly. Additionally, anthropogenic impacts on climatic factors could influence the dust emission indirectly. For instance, natural vegetation pattern can be well modified as a consequence of land use by human being, that will change surface features and soil properties thus lead to additional dust source regions. In order to better understand the effects of climate changes on atmospheric dust distribution, a long period model simulation is necessary and year-to-year databases

**Improved dust emission scheme in ECHAM5-HAM GCM**

T. Cheng et al.

Title Page

Abstract

Introduction

Conclusions

References

Tables

Figures

◀

▶

◀

▶

Back

Close

Full Screen / Esc

Printer-friendly Version

Interactive Discussion

of soil texture and vegetation cover will be needed.

*Acknowledgements.* We thank X. Xu and C. Prigent for their helps in providing maps of East-Asian soil texture and the global surface aerodynamic roughness length  $Z_0$ . Instructive discussions with S. Kloster and C. Reader are appreciated. Y. Peng was supported by the Alexander von Humboldt foundation in Germany. The model simulation and data storage were performed at DKRZ (German Climate Computing Centre).

## References

- Chadwick, O. A., Derry, L. A., Vitousek, P. M., Huebert, B. J., and Hedin, L. O.: Changing sources of nutrients during four million years of ecosystem development, *Nature*, 397, 491–497, 1999.
- Chatenet, B., Marticorena, B., Gomes, L., and Bergametti, G.: Assessing the microped size distributions of desert soils erodible by wind, *Sedimentology*, 43, 901–911, 1996.
- Ding, Z. L., Ren, J. Z., Yang, S. L., and Liu, T. S.: Climate instability during the penultimate glaciation: evidence from two high-resolution loess records, China, *J. Geophys. Res.*, 104, 20 123–20 132, 1999.
- Fécan, F., Marticorena, B., and Bergametti, G.: Parameterization of the increase of the aeolian erosion threshold wind friction velocity due to soil moisture for arid and semi-arid areas, *Ann. Geophys.*, 17, 149–157, 1999, <http://www.ann-geophys.net/17/149/1999/>.
- Gillette, D. A., Adams, J., Muhs, D., and Khil, R.: Threshold friction velocities and rupture moduli for crusted desert soil for the input of soil particles into the air, *J. Geophys. Res.*, 87, 9003–9016, 1982.
- Gillette, D. A. and Passi, R.: Modeling dust emission caused by wind erosion, *J. Geophys. Res.*, 93, 14 233–14 242, 1988.
- Ginoux, P., Chin, M., Tegen, I., et al.: Sources and distributions of dust aerosols simulated with the GOCART model, *J. Geophys. Res.*, 106, 20 255–20 273, 2001.
- Intergovernmental Panel on Climate Change: *Climate Change 2001*, edited by: Houghton, J. T., Ding, Y., Griggs, D. J., et al., Cambridge Univ. Press, New York, 2001.
- Kanai, Y., Ohta, A., Kamioka, H., et al.: Characterization of Aeolian dust in east China and Japan from 2001 to 2003, *J. Meteorol. Soc. Jpn.*, 83A, 73–106, 2005.

## Improved dust emission scheme in ECHAM5-HAM GCM

T. Cheng et al.

Title Page

Abstract

Introduction

Conclusions

References

Tables

Figures

◀

▶

◀

▶

Back

Close

Full Screen / Esc

Printer-friendly Version

Interactive Discussion

- Kim, K. H. and Kim, M. Y.: The effects of Asian dust on particulate matter fractionation in Seoul, Korea during spring 2001, *Chemosphere*, 51, 707–721, 2003.
- Kim, J. Y., Yoon, S. C., Kim, S. W., et al.: Chemical apportionment of shortwave direct aerosol radiative forcing at the Gosan super-site, Korea during ACE-Asia, *Atmos. Environ.*, 40, 6718–6729, 2006.
- 5 Kinne, S., Schulz, M., Textor, C., et al.: An AeroCom initial assessment-optical properties in aerosol component modules of global models, *Atmos. Chem. Phys.*, 6, 1815–1834, 2006, <http://www.atmos-chem-phys.net/6/1815/2006/>.
- Kinne, S., Lohmann, U., Feichter, J., Schulz, M., et al.: Monthly averages of aerosol properties: A global comparison among models, satellite data, and AERONET ground data, *J. Geophys. Res.*, 108, 4634, doi:10.1029/2001JD001253, 2003.
- 10 Laurent, B., Marticorena, B., Bergametti, G., et al.: Simulation of the mineral dust emission frequencies from desert areas of China and Mongolia using an aerodynamic roughness length map derived from the POLDER/ADEOS 1 surface products, *J. Geophys. Res.*, 110, D18S04, doi:10.1029/2004JD005013, 2005.
- 15 Laurent, B., Marticorena, B., Bergametti, G., and Mei, F.: Modeling mineral dust emissions from Chinese and Mongolian deserts, *Global Planet. Change*, 52, 121–141, 2006.
- Marticorena, B. and Bergametti, G.: Modeling the atmospheric dust cycle: 1. Design of a soil derived dust emission scheme, *J. Geophys. Res.*, 100, 16 415–16 430, 1995.
- 20 Marticorena, B., Bergametti, G., Aumont, B., et al.: Modeling the atmospheric dust cycle: 2. Simulations of Saharan dust sources, *J. Geophys. Res.*, 102, 4387–4404, 1997a.
- Marticorena, B., Bergametti, G., Gillette, D. A., and Belnap, J.: Factors controlling threshold friction velocity in semiarid and arid areas of the United States, *J. Geophys. Res.*, 102, 23 277–23 287, 1997b.
- 25 Marticorena, B., Chazette, P., Bergametti, G., Dulac, F., and Legrand, M.: Mapping the aerodynamic roughness length of desert surfaces from the POLDER/ADEOS bi-reflectance product, *Int. J. Remote Sens.*, 25, 603–626, 2004.
- Martin, J. H. and Fitzwater, S. E.: Iron deficiency limits phytoplankton growth in the north-east Pacific subarctic, *Nature*, 331, 341–343, 1988.
- 30 Mei, F., Zhang, X., Lu, H., Shen, Z., and Wang, Y.: Characterization of MASDs of surface soils in north China and its influence on estimating dust emission, *Chin. Sci. Bull.*, 49(20), 2169–2176, 2004.
- Middleton, N. J.: A geography of dust storms in south-west Asia, *J. Climatol.*, 6, 183–196,

---

**Improved dust emission scheme in ECHAM5-HAM GCM**T. Cheng et al.

---

Title Page

Abstract

Introduction

Conclusions

References

Tables

Figures

◀

▶

◀

▶

Back

Close

Full Screen / Esc

Printer-friendly Version

Interactive Discussion

1986.

Natsagdorj, L., Jugder, D., and Chung, Y. S.: Analysis of dust storms observed in Mongolia during 1937–1999, *Atmos. Environ.*, 37, 1401–1411, 2003.

Petit, J. R., Jouzel, J., Mounier, L., Korotkevich, Y. S., Kotlyakov, V. I. and Lorius, C.: Palaeoclimatological and chronological implications of the Vostok core dust record, *Nature*, 343, 56–58, 1990.

Petit, J. R., Jouzel, J., Raynaud, D., et al.: Climate and atmospheric history of the past 420 000 years from the Vostok ice core, Antarctica, *Nature*, 399, 429–436, 1999.

Prigent, C., Tegen, I., Aires, F., Marticorena, B., and Zribi, M.: Estimation of the aerodynamic roughness length in arid and semi-arid regions over the globe with the ERS scatterometer, *J. Geophys. Res.*, 110, D09205, doi:10.1029/2004JD005370, 2005.

Prospero, J. M.: Long-term measurements of the transport of African mineral dust to the southeastern United States: Implications for regional air quality, *J. Geophys. Res.*, 104(D13), 15917–15927, 1999.

Shao, Y., Yang, Y., Wang, J., et al.: Northeast Asian dust storms: Real-time numerical prediction and validation, *J. Geophys. Res.*, 108(D22), 4691, doi:10.1029/2003JD003667, 2003.

Sokolik, I. N. and Toon, O. B.: Direct radiative forcing by anthropogenic airborne mineral aerosols, *Nature*, 381, 681–683, 1996.

Solomon, P. A., Fall, T., Salmon, L., Cass, G. R., Gray, H. A., and Davision, A.: Chemical characteristics of PM10 aerosols collected in the Los Angeles Area, *JAPCA*, 39, 154–163, 1989.

Stier, P., Feichter, J., Kinne, S., et al.: The aerosol-climate model ECHAM5-HAM, *Atmos. Chem. Phys.*, 5, 1125–1156, 2005,  
<http://www.atmos-chem-phys.net/5/1125/2005/>.

Sun, J.: Provenance of loess material and formation of loess deposits on the Chinese Loess Plateau, *Earth Planet. Sci. Lett.*, 203, 845–859, 2002.

Tegen, I., Lacis, A. A., and Fung, I.: The influence on climate forcing of mineral aerosol from disturbed soils, *Nature*, 380, 419–422, 1996.

Tegen, I., Harrison, S. P., Kohfeld, K., Prentice, I. C., Coe, M., and Heimann, M.: Impact of vegetation and preferential source areas on global dust aerosol: Results from a model study, *J. Geophys. Res.*, 107(D21), 4576, doi:10.1029/2001JD000963, 2002.

Tegen, I., Werner, M., Harrison, S. P., and Kohfeld, K. E.: Relative importance of climate and land use in determining present and future global soil dust emission, *Geophys. Res. Lett.*,

ACPD

7, 13959–13987, 2007

## Improved dust emission scheme in ECHAM5-HAM GCM

T. Cheng et al.

Title Page

Abstract

Introduction

Conclusions

References

Tables

Figures

◀

▶

◀

▶

Back

Close

Full Screen / Esc

Printer-friendly Version

Interactive Discussion

EGU

- 31, L05105, doi:10.0129/2003GL019216, 2004.
- Timmreck, C. and Schulz, M.: Significant dust simulation differences in nudged and climatological operation mode of the AGCM ECHAM, *J. Geophys. Res.*, 109, D13202, doi:10.1029/2003JD004381, 2004.
- 5 Van Den Hurk, B., Viterbo, P., Beljaars, A. and Betts, A.: Offline validation of the ERA40 surface scheme, *ECMWF Tech Memo*, 295, 42 pp., 2000.
- Werner, M., Tegen, I., Harrison, S. P., et al.: Seasonal and interannual variability of the mineral dust cycle under present and glacial climate conditions, *J. Geophys. Res.*, 107(D1), 4001, doi:10.1029/2002JD002365, 2002.
- 10 Xu, X., Levy, J. K., Lin, Z., and Chen, H.: An investigation of sand-dust storm events and land surface characteristics in China using NOAA NDVI data, *Global Planet. Change*, 52, 182–196, 2006.
- Yabuki, S., Mikami, M., Nakamura, Y., et al.: The characteristics of atmospheric aerosol at Aksu, an Asian dust-source region of North-West China: A summary of observations over the three years from March 2001 to April 2004, *J. Meteorol. Soc. Jpn*, 83A, 45–72, 2005.
- 15 Yang, G., Xiao, H., and Tuo, W.: Black windstorm in northwest China: a case study of the strong sand-dust storm on May 5th 1993, *Global Alarm: Dust and Sandstorms from the World's Drylands*, United Nations: Bangkok, Thailand, pp 49–73, 2001.
- Zha, Y. and Gao, J.: Characteristics of desertification and its rehabilitation in China, *J. Arid Environ.*, 37, 419–432, 1997.
- 20 Zhang, X. Y., Gong, S. L., Shen, Z. X., et al.: Characterization of soil dust aerosol in China and its transport and distribution during 2001 ACE-Asia: 1. Network observations, *J. Geophys. Res.* 108(D9), 4261, doi:10.1029/2002JD002632, 2003.
- Zobler, L.: A world soil file for global climate modeling, *NASA Tech. Memo*, 87802, 32 pp., 25 1986.

---

**Improved dust emission scheme in ECHAM5-HAM GCM**T. Cheng et al.

---

[Title Page](#)[Abstract](#)[Introduction](#)[Conclusions](#)[References](#)[Tables](#)[Figures](#)[◀](#)[▶](#)[◀](#)[▶](#)[Back](#)[Close](#)[Full Screen / Esc](#)[Printer-friendly Version](#)[Interactive Discussion](#)

## Improved dust emission scheme in ECHAM5-HAM GCM

T. Cheng et al.

**Table 1.** Statistical parameters (MMD,  $\sigma$ , P) of mass-size log-normal distribution in fine and coarse modes, clay and silt contents, ratio of the vertical to horizontal dust fluxes ( $\alpha$ ) and residual soil moisture ( $w'$ ) for the 5 updated soil types in East-Asian dust source areas.

|                      | Fine mode                      |            |                       | Coarse mode                    |            |                       | Clay<br>[%] | Silt<br>[%] | $\alpha$<br>[cm <sup>-1</sup> ] | $w'$ |
|----------------------|--------------------------------|------------|-----------------------|--------------------------------|------------|-----------------------|-------------|-------------|---------------------------------|------|
|                      | MMD <sub>1</sub><br>[ $\mu$ m] | $\sigma_1$ | P <sub>1</sub><br>[%] | MMD <sub>2</sub><br>[ $\mu$ m] | $\sigma_2$ | P <sub>2</sub><br>[%] |             |             |                                 |      |
| Taklimakan           | 84                             | 1.5        | 85                    | 442                            | 1.5        | 3                     | 2           | 11          | 1.9e-06                         | 0.12 |
| Loess                | 70                             | 1.5        | 33                    | 450                            | 1.5        | 0                     | 17          | 50          | 1.9e-04                         | 0.15 |
| Gobi                 | 86                             | 1.5        | 22                    | 457                            | 1.8        | 31                    | 12          | 34          | 3.9e-05                         | 0.13 |
| Desert and sand land | 101                            | 1.5        | 41                    | 305                            | 1.5        | 46                    | 3           | 10          | 2.8e-06                         | 0.12 |
| Other mixture soils  | 90                             | 1.5        | 16                    | 293                            | 1.8        | 39                    | 10          | 35          | 3.1e-05                         | 0.13 |

Title Page

Abstract

Introduction

Conclusions

References

Tables

Figures

◀

▶

◀

▶

Back

Close

Full Screen / Esc

Printer-friendly Version

Interactive Discussion

## Improved dust emission scheme in ECHAM5-HAM GCM

T. Cheng et al.

**Table 2.** Reference and six sensitivity simulations of ECHAM5-HAM for the year 2000: global annual mean of dust emission amount, atmospheric dust burden, total aerosol optical thickness (AOT) and dust AOT.

| Case | East-Asian soil properties | Surface roughness length $Z_0$ | Residual soil moisture $w'$ | Wind stress correction factor | Dust emission [ $\text{Tg yr}^{-1}$ ] | AOT  | Dust AOT | Dust burden [ $\text{Tg}$ ] |
|------|----------------------------|--------------------------------|-----------------------------|-------------------------------|---------------------------------------|------|----------|-----------------------------|
| 0    | No                         | No                             | No                          | 0.86                          | 736                                   | 0.13 | 0.0118   | 9.78                        |
| 1    | No                         | Yes                            | No                          | 0.86                          | 173                                   | 0.12 | 0.0030   | 2.49                        |
| 2    | No                         | No                             | Yes                         | 0.86                          | 719                                   | 0.13 | 0.0116   | 9.64                        |
| 3    | Yes                        | No                             | No                          | 0.86                          | 858                                   | 0.13 | 0.0128   | 10.48                       |
| 4    | Yes                        | Yes                            | Yes                         | 0.86                          | 205                                   | 0.12 | 0.0032   | 2.70                        |
| 5    | Yes                        | Yes                            | Yes                         | 0.56                          | 1671                                  | 0.15 | 0.0292   | 23.60                       |
| 6    | No                         | No                             | No                          | 0.56                          | 3476                                  | 0.18 | 0.0567   | 46.00                       |

Title Page

Abstract

Introduction

Conclusions

References

Tables

Figures

◀

▶

◀

▶

Back

Close

Full Screen / Esc

Printer-friendly Version

Interactive Discussion

**Table 3.** List of annual mean surface dust concentration ( $\mu\text{g m}^{-3}$ ) used in Fig. 4: measurements are taken from global remote marine sites by University of Miami network. Model results in the corresponding site are taken from simulations of year 2000 with the original and improved dust emission scheme (case 0 and case 5) respectively.

| Location                    | Longitude | Latitude | Measurement | Case 0 | Case 5 |
|-----------------------------|-----------|----------|-------------|--------|--------|
| Cape Point – South Africa   | 18.5      | −34.3    | 2.20        | 0.28   | 0.13   |
| Marsh – King George Island  | −58.3     | −62.2    | 0.52        | 0.0008 | 0.0008 |
| Mawson – Antarctica         | 62.5      | −67.6    | 0.10        | 0.0002 | 0.0002 |
| Palmer Station – Antarctica | −64.1     | −64.8    | 0.35        | 0.0002 | 0.0001 |
| Yate – New Caledonia        | 167.0     | −22.1    | 0.17        | 0.45   | 0.56   |
| Funafuti – Tuvalu           | −179.2    | −8.5     | 0.19        | 0.006  | 0.02   |
| Nauru                       | 166.9     | −0.5     | 0.10        | 0.007  | 0.03   |
| Norfolk Island              | 168.0     | −29.1    | 0.84        | 0.52   | 0.75   |
| Rarotonga – Cook Islands    | −159.8    | −21.2    | 0.11        | 0.069  | 0.14   |
| American Samoa              | −170.6    | −14.2    | 0.16        | 0.0045 | 0.006  |
| Midway Island               | −177.4    | 28.2     | 0.72        | 0.054  | 0.15   |
| Oahu Hawaii                 | −157.7    | 21.3     | 0.66        | 0.023  | 0.063  |
| Cheju – South Korea         | 126.5     | 33.5     | 14.14       | 7.75   | 14.11  |
| Hedo Okinawa – Japan        | 128.2     | 26.9     | 8.37        | 3.30   | 6.57   |
| Fanning Island              | −159.3    | 3.9      | 0.10        | 0.0063 | 0.02   |
| Enewetak Atoll              | 162.3     | 11.3     | 0.24        | 0.008  | 0.03   |
| Barbados                    | −59.4     | 13.2     | 14.48       | 7.70   | 14.62  |
| Izana Tenerife              | −16.5     | 28.3     | 30.18       | 20.55  | 43.38  |
| Bermuda                     | −64.9     | 32.3     | 3.36        | 0.85   | 1.64   |
| Mace Head – Ireland         | −9.9      | 53.3     | 1.00        | 0.28   | 0.67   |
| Miami                       | −80.2     | 25.8     | 4.59        | 2.08   | 3.78   |
| Average                     | –         | –        | 3.93        | 2.09   | 4.13   |

## Improved dust emission scheme in ECHAM5-HAM GCM

T. Cheng et al.

Title Page

Abstract

Introduction

Conclusions

References

Tables

Figures

◀

▶

◀

▶

Back

Close

Full Screen / Esc

Printer-friendly Version

Interactive Discussion

**Table 4.** List of monthly mean near-surface dust concentration ( $\text{mg m}^{-3}$ ) used in Fig. 6. Measurements are collected from in-situ observations in northern Asia. Model results in the corresponding site and period are taken from simulations of year 2000 with the original and improved dust emission scheme (case 0 and case 5) respectively.

| Site location          | Latitude | Longitude | Period  | Measurement | Case 0 | Case 5 | Reference            |
|------------------------|----------|-----------|---------|-------------|--------|--------|----------------------|
| Aksu – China           | 40.27    | 80.47     | 2001.03 | 0.081       | 0.064  | 0.084  | Yabuki et al. (2005) |
|                        |          |           | 2001.05 | 0.417       | 0.021  | 0.118  | Zhang et al. (2003)  |
|                        |          |           | 2002.03 | 0.531       | 0.081  | 0.245  | Yabuki et al. (2005) |
|                        |          |           | 2002.04 | 0.597       | 0.145  | 0.561  |                      |
| Dunhuang – China       | 40.50    | 94.82     | 2002.05 | 0.179       | 0.012  | 0.036  |                      |
|                        |          |           | 2001.05 | 0.212       | 0.009  | 0.026  | Zhang et al. (2003)  |
|                        |          |           | 2002.04 | 0.157       | 0.026  | 0.087  | Shao et al. (2003)   |
|                        |          |           | 2001.03 | 0.304       | 0.060  | 0.104  | Zhang et al. (2003)  |
| Zhenbeitai – China     | 38.29    | 109.70    | 2001.04 | 0.209       | 0.199  | 0.347  |                      |
|                        |          |           | 2001.05 | 0.127       | 0.031  | 0.050  |                      |
|                        |          |           | 2001.03 | 0.170       | 0.025  | 0.053  | Zhang et al. (2003)  |
| Changwu – China        | 35.02    | 107.68    | 2001.04 | 0.211       | 0.079  | 0.215  |                      |
|                        |          |           | 2001.05 | 0.057       | 0.022  | 0.043  |                      |
|                        |          |           | 2001.03 | 0.328       | 0.013  | 0.029  | Zhang et al. (2003)  |
| Lanzhou – China        | 36.05    | 103.88    | 2001.04 | 0.305       | 0.060  | 0.162  |                      |
|                        |          |           | 2001.05 | 0.164       | 0.026  | 0.042  |                      |
|                        |          |           | 2001.03 | 0.470       | 0.022  | 0.047  | Zhang et al. (2003)  |
| Shapotou – China       | 37.50    | 105.00    | 2001.04 | 0.370       | 0.143  | 0.389  |                      |
|                        |          |           | 2001.05 | 0.157       | 0.033  | 0.077  |                      |
|                        |          |           | 2002.04 | 0.111       | 0.039  | 0.082  | Shao et al. (2003)   |
| Inner Mongolia – China | 42.67    | 115.95    | 2001.04 | 0.447       | 0.197  | 0.474  | Cheng et al. (2005)  |
|                        |          |           | 2001.03 | 0.252       | 0.054  | 0.128  | Zhang et al. (2003)  |
| Beijing – China        | 39.93    | 116.35    | 2001.04 | 0.206       | 0.142  | 0.257  |                      |
|                        |          |           | 2001.05 | 0.133       | 0.061  | 0.096  |                      |
|                        |          |           | 2002.03 | 0.282       | 0.058  | 0.113  | Kanai et al. (2005)  |
|                        |          |           | 2002.04 | 0.267       | 0.071  | 0.169  |                      |
| Qingdao – China        | 36.07    | 120.33    | 2001.05 | 0.026       | 0.020  | 0.041  | Kanai et al. (2005)  |
|                        |          |           | 2002.03 | 0.083       | 0.056  | 0.098  |                      |
|                        |          |           | 2002.04 | 0.055       | 0.042  | 0.095  |                      |
| Hefei – China          | 31.90    | 117.16    | 2002.03 | 0.066       | 0.042  | 0.072  | Kanai et al. (2005)  |
|                        |          |           | 2001.03 | 0.113       | 0.016  | 0.044  | Kim et al. (2006)    |
| Seoul – South Korea    | 37.53    | 127.07    | 2001.04 | 0.093       | 0.038  | 0.100  |                      |
|                        |          |           | 2001.05 | 0.076       | 0.006  | 0.026  |                      |
|                        |          |           | 2001.04 | 0.052       | 0.031  | 0.056  | Kim et al. (2003)    |
| Gosan – South Korea    | 33.29    | 126.16    | 2001.03 | 0.035       | 0.004  | 0.011  | Kanai et al. (2005)  |
|                        |          |           | 2001.04 | 0.036       | 0.008  | 0.033  |                      |
|                        |          |           | 2001.05 | 0.029       | 0.005  | 0.011  |                      |
|                        |          |           | 2002.03 | 0.049       | 0.016  | 0.029  |                      |
| Tsukuba – Japan        | 36.06    | 140.14    | 2002.04 | 0.049       | 0.014  | 0.036  |                      |
|                        |          |           | 2001.03 | 0.034       | 0.006  | 0.015  | Kanai et al. (2005)  |
|                        |          |           | 2001.04 | 0.038       | 0.010  | 0.039  |                      |
|                        |          |           | 2001.05 | 0.027       | 0.006  | 0.013  |                      |
| Nagoya – Japan         | 35.15    | 136.96    | 2002.03 | 0.030       | 0.011  | 0.033  |                      |
|                        |          |           | 2002.04 | 0.054       | 0.019  | 0.048  |                      |
|                        |          |           | 2001.05 | 0.045       | 0.004  | 0.022  | Kanai et al. (2005)  |
|                        |          |           | 2002.03 | 0.062       | 0.017  | 0.046  |                      |
| Fukuoka – Japan        | 33.55    | 130.37    | 2002.04 | 0.060       | 0.028  | 0.066  |                      |
|                        |          |           | 2002.03 | 0.033       | 0.005  | 0.012  | Kanai et al. (2005)  |
|                        |          |           | 2002.04 | 0.046       | 0.007  | 0.020  |                      |
| Naha – Japan           | 26.20    | 127.69    |         |             |        |        |                      |
| Average                | –        | –         | –       | 0.162       | 0.043  | 0.102  | –                    |

## Improved dust emission scheme in ECHAM5-HAM GCM

T. Cheng et al.

Title Page

Abstract

Introduction

Conclusions

References

Tables

Figures

◀

▶

◀

▶

Back

Close

Full Screen / Esc

Printer-friendly Version

Interactive Discussion

**Improved dust emission scheme in ECHAM5-HAM GCM**

T. Cheng et al.

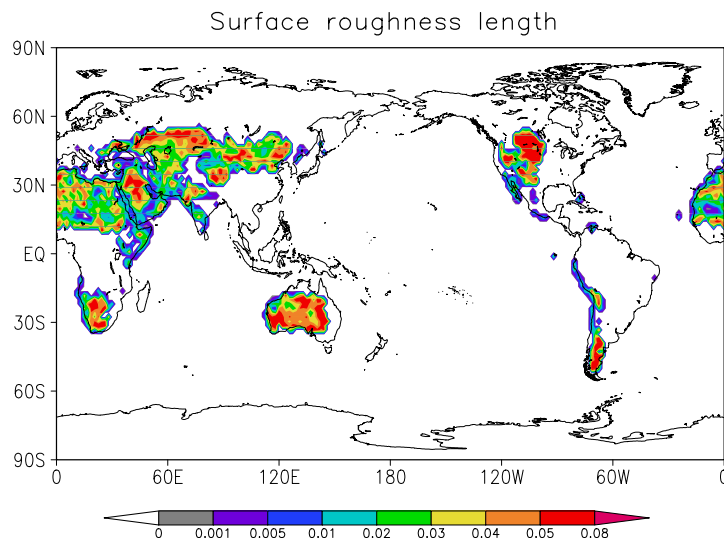


**Fig. 1.** Updated annual mean field of aerodynamic surface roughness length  $Z_0$  (cm) with a horizontal resolution of  $1.8^\circ \times 1.8^\circ$  (Prigent et al., 2005). Data are shown only in arid and semi-arid areas of the globe, forests and dense vegetated regions are excluded because they are not potential dust source areas.

[Title Page](#)[Abstract](#)[Introduction](#)[Conclusions](#)[References](#)[Tables](#)[Figures](#)[◀](#)[▶](#)[◀](#)[▶](#)[Back](#)[Close](#)[Full Screen / Esc](#)[Printer-friendly Version](#)[Interactive Discussion](#)

## Improved dust emission scheme in ECHAM5-HAM GCM

T. Cheng et al.

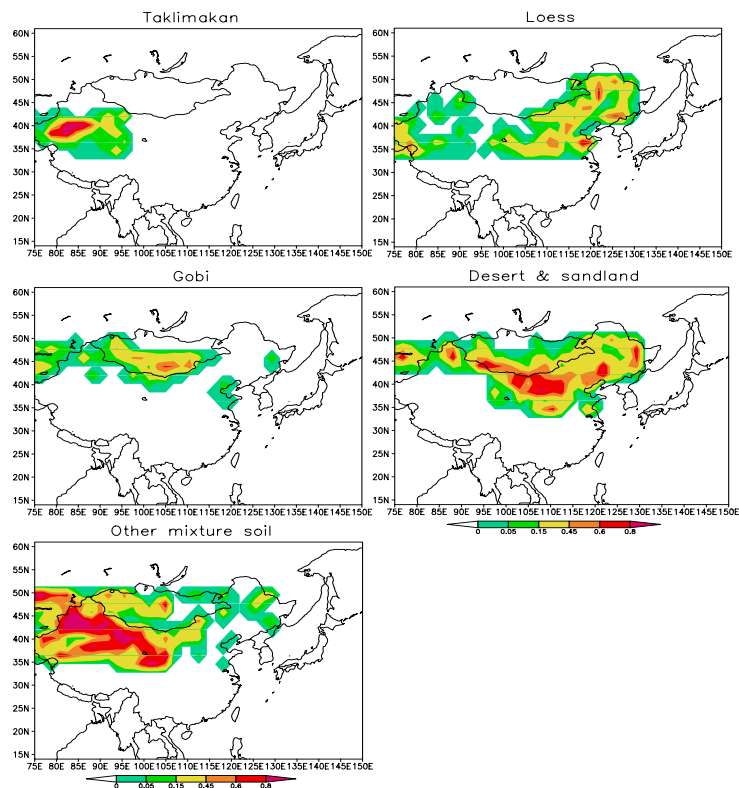


**Fig. 2.** Area percentages of 5 updated soil types in East-Asian dust source areas with a horizontal resolution of  $1.8^\circ \times 1.8^\circ$ .

[Title Page](#)[Abstract](#)[Introduction](#)[Conclusions](#)[References](#)[Tables](#)[Figures](#)[◀](#)[▶](#)[◀](#)[▶](#)[Back](#)[Close](#)[Full Screen / Esc](#)[Printer-friendly Version](#)[Interactive Discussion](#)

## Improved dust emission scheme in ECHAM5-HAM GCM

T. Cheng et al.

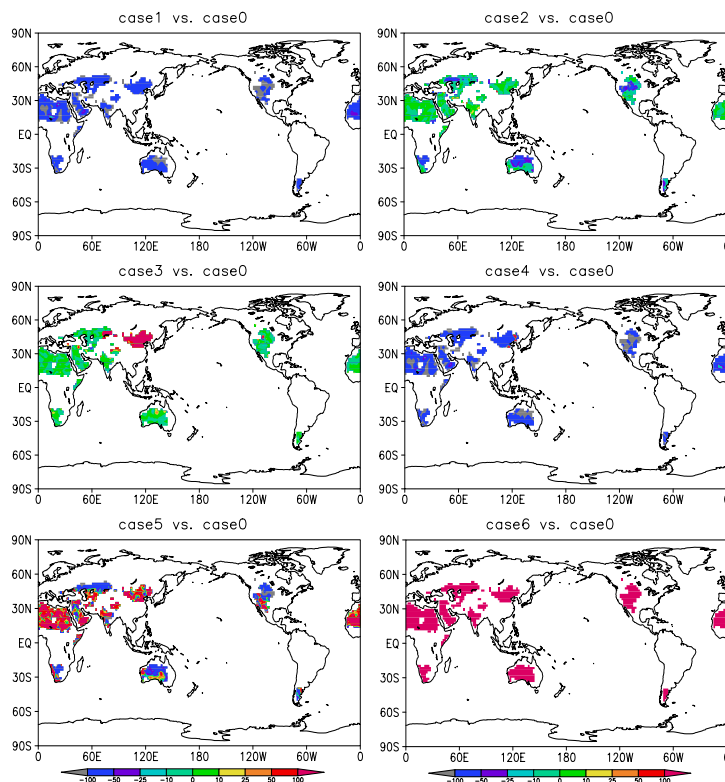


**Fig. 3.** Percentage differences (%) between sensitivity simulations and the reference simulation in terms of the annual mean dust emission amount ( $\text{Tgyr}^{-1}$ , global mean values are listed in column 6 of Table 2).

[Title Page](#)[Abstract](#)[Introduction](#)[Conclusions](#)[References](#)[Tables](#)[Figures](#)[◀](#)[▶](#)[◀](#)[▶](#)[Back](#)[Close](#)[Full Screen / Esc](#)[Printer-friendly Version](#)[Interactive Discussion](#)



## Improved dust emission scheme in ECHAM5-HAM GCM

T. Cheng et al.

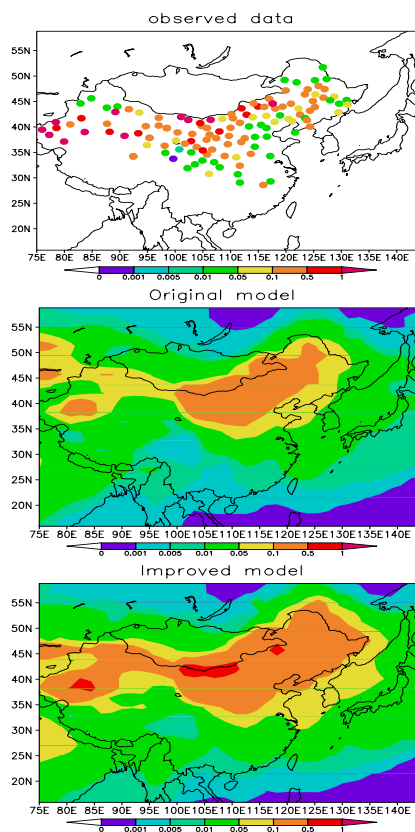


**Fig. 5.** A comparison of monthly mean surface dust concentration ( $\text{mg m}^{-3}$ ) in East Asia for April, 2001. The observed data are derived from visibility. Dust concentrations between  $0.001$  and  $1 \text{ mg m}^{-3}$  as indicated in the color bar are corresponding to visibilities of 69.2, 54.7, 48.4, 33.8, 27.5, 12.8 and 6.5 km respectively (Shao et al., 2003). Model results are taken from simulations with the original and improved dust emission scheme (case 0 and case 5) respectively.

[Title Page](#)[Abstract](#)[Introduction](#)[Conclusions](#)[References](#)[Tables](#)[Figures](#)[◀](#)[▶](#)[◀](#)[▶](#)[Back](#)[Close](#)[Full Screen / Esc](#)[Printer-friendly Version](#)[Interactive Discussion](#)

**Improved dust emission scheme in ECHAM5-HAM GCM**

T. Cheng et al.

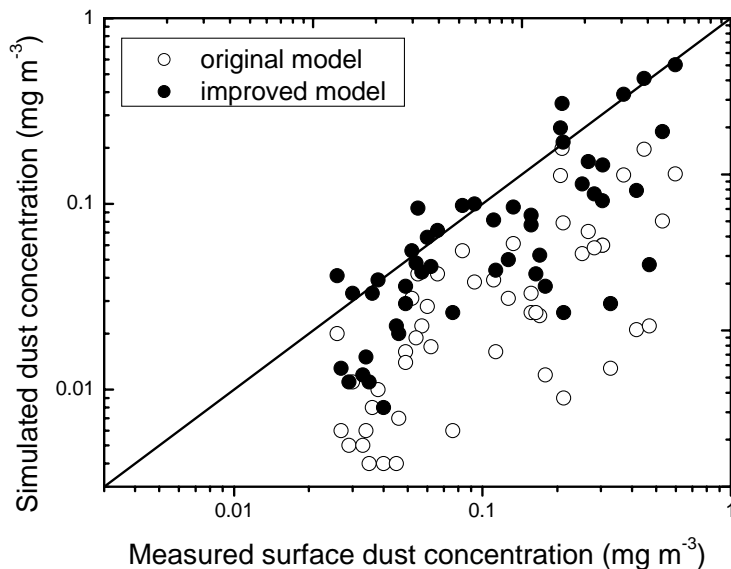


**Fig. 6.** A comparison of monthly mean surface dust concentration between measurements at Asian sites and corresponding model results. Data, locations and time period are listed in Table 4. Solid line is the 1 to 1 line. Logarithm scale is used in order to show some low values of model results. Correlation coefficients of original and improved models are 0.56 and 0.71 respectively.

[Title Page](#)[Abstract](#)[Introduction](#)[Conclusions](#)[References](#)[Tables](#)[Figures](#)[◀](#)[▶](#)[◀](#)[▶](#)[Back](#)[Close](#)[Full Screen / Esc](#)[Printer-friendly Version](#)[Interactive Discussion](#)